Composites Part A: Applied Science and Manufacturing
April 2024, Volume 179, Pages 108027 (9p.)
https://doi.org/10.1016/j.compositesa.2024.108027
https://archimer.ifremer.fr/doc/00872/98401/

Basalt fibre degradation in seawater and consequences for long term composite reinforcement

Le Gué Louis [1, 2, *], Davies Peter [1], Arhant Mael [1], Vincent Benoit [2], Verbouwe Wouter [3]

[1] Ifremer RDT, Research and Technology Development Unit, 1625 route de Sainte-Anne, Plouzané, 29280, France
[2] DECOD (Ecosystem Dynamics and Sustainability), IFREMER, INRAE, Institut Agro, Lorient, 56325, France
[3] Basaltex, Zuidstraat 18, Wevelgem, 8560, Belgium

* Corresponding author : Louis Le Gué, email address : louis.le.gue@ifremer.fr

Abstract :

Basalt fibres are increasingly employed as reinforcements in marine composites, but their behaviour in natural marine environments is underexplored. This study investigates basalt fibre ageing in renewed natural seawater at 15 °C and 40 °C. After one month in seawater at 15 °C and 40 °C, tensile strength dropped, stabilizing at approximately −40% and −60%, respectively. This rapid initial property decline, followed by slower degradation, is attributed to an altered surface layer on the fibres. Initially causing significant property loss, this layer then plays a protective role, preserving the fibre core. The impact on basalt/epoxy composites exposed to 7.5 years of seawater was less severe, with a 20% loss at 40 °C, demonstrating the protective function of the matrix. This study suggests that basalt fibres undergo rapid, then stable, property degradation in water, but remain suitable for use as epoxy matrix composite reinforcements, thanks to the protective role of the resin.

Graphical abstract

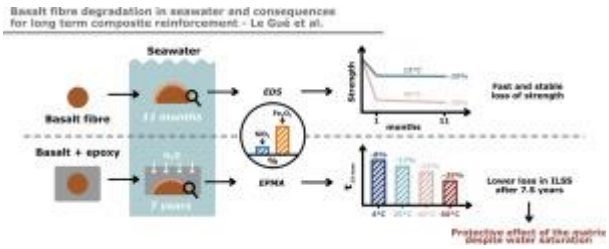

Highlights

► Basalt fibres were immersed in seawater for up to 11 months. ► Basalt/epoxy composites were exposed to seawater for 7.5 years. ► The fibres alone experienced rapid property loss, followed by stabilization. ► Immersed fibres displayed a degraded surface layer rich in iron oxide and low in silicon oxide. ► For composite samples the protective role of the epoxy matrix resulted in minimal strength loss.

Keywords : basalt fibres, composites, seawater ageing

1. Introduction

In recent years, the marine industry has been actively engaged in an ecological transition to reduce its environmental impact. This shift involves adopting more environmentally-friendly practices, including the exploration of alternative materials with lower ecological footprints compared to conventional ones.

Within this context, the utilization of basalt fibres as a substitute for glass fibres for composites is gaining popularity in boatbuilding, despite the lack of comprehensive data on the life cycle inventory of individual fibres in the scientific literature. However, as the properties of these fibres are inferior to those of carbon fibres, they are not intended to replace them (Chowdhury et al., 2022). Current applications of basalt fibres range from the reinforcement of polymers in the automotive industry (Wang et al., 2021b), to the reinforcement of cement in civil engineering (Sim et al., 2005). Basalt fibres are produced through the grinding and extrusion of volcanic rock resulting from the rapid cooling of magma in the ocean (Militky

et al., 2002). While the composition of basalt is similar to glass, it contains iron oxides in addition to silica, which affects the final properties of the fibres (Fiore et al., 2015; Austin and Subramanian, 1979). However, the presence of iron in the fibres also leads to interactions between their surfaces and the surrounding environment as described by several authors (Burkhard and Scherer, 2006; Wei et al., 2011). The marine environment is known for its challenging conditions, with high concentrations of ions (Millero et al., 2008), making basalt fibres susceptible to degradation. Table 1 presents a list of published studies on the ageing of basalt fibres or basalt composites in different aqueous environments.

Reference	sample type	ageing environment	ageing temp.	max ageing time	year
(Scheffler et al., 2009)	fibres	alkaline	20, 40, 60, 80°C	15 days	2009
(Wei et al., 2011)	composite	artificial seawater	25°C	3 months	2011
(Förster et al., 2014)	fibres	alkaline	80°C	11 days	2014
(Wu et al., 2015)	fibres + composite	alkaline, acidic, saltwater, tap water	25, 55°C	66 days	2015
(Rybin et al., 2016)	composite	alkaline	"ambient"	64 days	2016
(Quagliarini et al., 2016)	composite	alkaline, acidic	100°C	3 hours	2016
(Davies and Verbouwe, 2018)	composite	natural seawater	4, 25, 40, 60°C	200 days	2018
(Tang et al., 2018)	fibres	alkaline	25, 50, 70°C	3 days	2018
(Wang et al., 2019)	composite	artificial seawater	25°C	6 weeks	2019
(Lu et al., 2020)	composite	alkaline, tap water, artificial seawater	20°C	180 days	2020
(Wang et al., 2021a)	fibres	artificial seawater	80, 85, 90°C	168 hours	2021
(Lu et al., 2022)	fibres + composite	artificial seawater, distilled water	20, 40, 60°C	90 days	2022

Table 1: List of published studies on the ageing of basalt fibres or basalt composites in different aqueous environments.

Basalt fibres are often depicted as alternative fibres in civil engineering and cement composites (Fiore et al., 2015; Jiang et al., 2022), which explains why the majority of ageing studies in the Table 1 refer to their durability in alkaline solutions (Scheffler et al., 2009; Förster et al., 2014; Wu et al., 2015; Rybin et al., 2016; Quagliarini et al., 2016; Tang et al., 2018). Fibre degradation was observed after immersion in both NaOH solutions (Scheffler et al., 2009; Förster et al., 2014; Wu et al., 2015; Rybin et al., 2016; Quagliarini et al., 2016; Tang et al., 2018) and CaOH solutions (Quagliarini et al., 2016). Some authors stated that the degradation was linked to the dissolution of the glass network during ageing (Scheffler et al., 2009; Förster et al., 2014). This degradation could be slowed down by the formation of a corrosion shell at the surface of the fibre (Förster et al., 2014; Tang et al., 2018) which is a temperature dependant process (Tang et al.,

2018). Fibres can also be protected inside a polymer matrix (Quagliarini et al., 2016), but the corrosion of the surface could degrade the fiber-matrix interfaces, leading to a loss of mechanical properties of the composite (Wu et al., 2015).

Saltwater and artificial seawater ageing has also been applied to basalt fibres (Wang et al., 2021a; Lu et al., 2022) and their composites (Wei et al., 2011; Wang et al., 2019, 2021a; Lu et al., 2022). Wang et al. (2021a) immersed basalt fibres in artificial seawater at high temperatures and first noticed a fast increase in the mechanical properties followed by a decrease. The authors stated that the increase was due to the smoothing of the micro-cracks present at the surface of the fibres due to the corrosion of the crack tips. The decrease was attributed to the glass network degradation by corrosion. After immersing basalt fibres in artificial seawater at lower temperatures, Lu et al. (2022) also observed an important decrease in the mechanical properties, without giving further details on the degradation process. Different authors showed that using a polymer matrix could protect the fibres from the degradation process (Quagliarini et al., 2016; Lu et al., 2022) which explains the enhanced durability observed at the composite scale in other studies (Wei et al., 2011; Davies and Verbouwe, 2018; Wang et al., 2019). However, basalt fibre reinforced composites are considered more sensitive to water uptake than glass fiber composites (Davies and Verbouwe, 2018; Lu et al., 2022). While some authors stated that the long term response of both composites are similar (Wei et al., 2011; Davies and Verbouwe, 2018), other observed a poorer resistance to seawater ageing for the basalt composite (Lu et al., 2020) due to the formation of a corrosion layer that degrades the fiber-matrix interface adhesion (Wang et al., 2019).

More generally this table highlights the increasing interest in basalt fibres in recent years, as most of the studies listed are less than 10 years old. The only study conducted in natural seawater with a substantial ageing period involves composites immersed for up to 200 days (Davies and Verbouwe, 2018). Furthermore, the other studies examining the ageing of basalt fibres alone in seawater were conducted using artificial seawater (Wang et al., 2021a; Lu et al., 2022). The present study aims first to characterize the long-term behaviour of basalt fibres in natural seawater at 15°C, close to the average temperature of the ocean, and at 40°C to facilitate the observation of degradation processes. These fibres are intended for integration into a resin, leading to the testing of a basalt/epoxy composite after 7.5 years of immersion in seawater at different temperatures to assess its very long-term ageing, and compare it to a reference glass/epoxy composite with the same matrix.

2. Materials & methods

2.1. Materials

Two types of samples were studied here: continuous basalt fibres alone and two composites.

Continuous basalt yarns were supplied by Basaltex, a basalt fibres supplier based in Belgium. The physical properties of the yarn are presented in Table 2. No additives were added during the manufacturing process.

Density $[g.cm^{-3}]$	2.67
Tex $[g.km^{-1}]$	320.4
Diameter $[\mu m]$	10 – 15

Table 2: Physical properties of as received yarns.

Two different composite panels were supplied by Basaltex: one made of continuous basalt fibres, one made of continuous glass fibres, and both with the same epoxy resin. The dimensions of the panels were 500x500 mm^2 with a thickness of 3 mm. The detailed constructions of both composites are presented in Table 3. The same matrix was used for both composites in order to compare the effect of the seawater ageing upon the different fibres. Panels were obtained by infusion by the Sirris company (Brussels, Belgium) and then post-cured 2 hours at 50°C and 2.5 hours at 80°C with ramps of 30 minutes between each step. These composites are the same as those studied by Davies and Verbouwe (2018).

	Fibres	Matrix
basalt/epoxy	Basaltex - BAS UNI 350 0° - 357 $g.m^{-2}$ / 90° 50 $g.m^{-2}$ + stitching 9 $g.m^{-2}$	Epoxy Araldite 1564 LY + Aradur 3687
E-glass/epoxy	Selcom - UNIE 300 0° - 300 $g.m^{-2}$ / 90° 60 $g.m^{-2}$ + stitching 13 $g.m^{-2}$	Epoxy Araldite 1564 LY + Aradur 3687

Table 3: Details on studied composites.

2.2. Ageing

The two types of samples, fibres alone and composites, were immersed in tanks filled with natural seawater. Yarn samples were wound around a polypropylene cylinder to avoid entangling during retrievals, and then placed inside a polypropylene pot. Composite panels were also placed in polypropylene pots for ageing. Plastic pots were then placed in the different ageing tanks. The seawater was pumped from Brest estuary and continuously renewed, providing a good representation of the conditions that the materials might experience in the marine environment. The tanks were maintained at various temperatures. The fibres alone were immersed in tanks regulated at 15°C and 40°C. The composite samples were immersed at 4°C, 25°C, 40°C and 60°C. Temperatures higher than those that materials may encounter in the marine

environment make it easier to observe certain physico-chemical degradation phenomena. Samples of fibres alone were removed after, 1, 3, and 7 months for tensile testing, while composite samples were removed for weighing over a period of seven and a half years, after which they were tested in interlaminar shear.

To gain a better understanding of the degradation of basalt fibres in an aqueous environment, ageing tests were also carried out using water deionized by osmosis, in order to assess the effect of ageing without specific ions present in seawater.

2.3. Mechanical testing

Yarns were tensile tested before and after ageing on an Instron™ 10 kN capacity test machine equipped with Instron™ pneumatic grips designed for yarn testing. The tests were controlled by setting a displacement speed of 50 mm/min. Strain was measured by following two markers with a Basler™ camera. All the tests were conducted in a room maintained at 21°C and 50% relative humidity. 20 samples were tested for the initial state, and 3 samples were tested for each ageing condition.

Composites were tested according to the ASTM D2344 standard to evaluate their interlaminar shear strength (ILSS). Samples were tested after 7.5 years of ageing in a saturated state, and their inter-laminar shear strengths were calculated according to Equation 1.

$$\tau_{13} = \frac{3}{4}\frac{F_{max}}{B * d} \tag{1}$$

Where τ_{13} is the inter-laminar shear stress at failure, Fmax is the maximum load measured during testing, B is the width, and d the thickness of the sample.

2.4. Surface characterization

Samples were observed by Scanning Electron Microscopy (SEM) using FEI Quanta 200 equipment. They were coated with a 60% gold / 40% palladium coating.

2.5. Composition analysis

Energy Dispersive Spectroscopy (EDS) has been used alongside SEM observations for qualitative interpretation of the observations. For a quantitative analysis, a CAMECA SX100 Electron Probe Microanalyser (EPMA) has been used on polished cross-sections (polished down to 0.25 micron grain size) coated with a carbon coating.

3. Results

3.1. Yarn

3.1.1. Initial state characterization

Twenty samples of the basalt yarn were tested, Figure 1 shows the stress-strain curves obtained. With a mean strain at break of 1.7%, a mean stress at break of 1457 MPa, and a mean modulus of 89.8 GPa, the

fibres exhibit a brittle behaviour common for mineral fibres. Table 4 summarizes the properties obtained from the test on the basalt fibres, together with properties for E-glass fibres taken from the literature (Xing et al., 2019). Basalt fibres and glass fibres have equivalent properties, with basalt fibres being slightly stiffer and E-glass fibres having a higher stress at break.

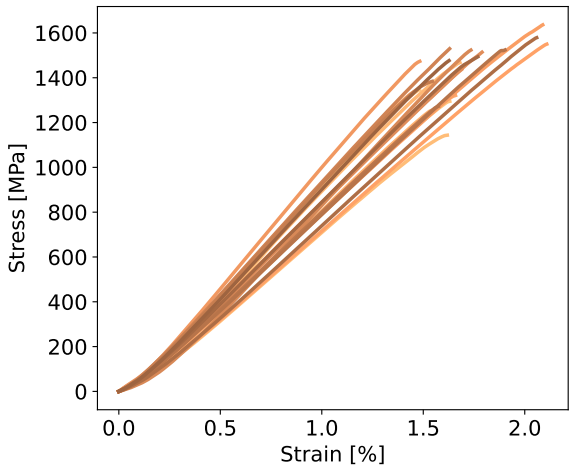

Figure 1: Initial tensile stress curves for basalt yarns.

	E [GPa]	$\epsilon_{failure}$ [%]	$\sigma_{failure}$ [MPa]
Basalt	77 – 106	1.5 – 2.1	1164 – 1669
E-glass	65.9 – 75.1	1.24 – 1.64	1280 – 2120

Table 4: Basalt and E-glass fibre properties (Xing et al., 2019).

3.1.2. Aged yarn sample testing

Basalt fibres samples were aged in tanks and retrieved after 1 month, 3 months, and 7 months. Three samples were tested for each condition without drying. Figure 2 shows the change in strength for samples aged at 15°C in seawater, 40°C in seawater, and 40°C in deionized water. The error bars represent the dispersion for each condition. After one month in 15°C seawater, basalt fibres have lost nearly 40% of their initial strength. This loss then stabilizes at a strength 45% lower after 7 months. The loss after one month at 40°C in seawater is more significant with a decrease in the strength of 86% and a stabilization around 70% of the unaged value. In deionized water the loss is equivalent to that in seawater with a stabilization around 70% reduction.

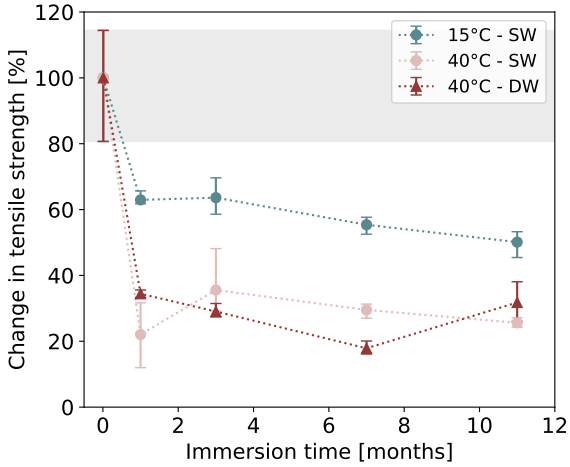

Figure 2: Change in strength for basalt yarn after different immersion times.

Immersion time [months]	1	3	7	11
15°C - seawater	-37%	-36%	-45%	-50%
40°C - seawater	-86%	-64%	-70%	-74%
40°C - deionized water	-66%	-82%	-71%	-68%

Table 5: Loss in strength for basalt yarns after different immersion times.

3.1.3. Surface characterization

After ageing, a change in the colour of the basalt fibre samples was observed which is shown in Figure 3. The filament in its initial state is a very dark brown, almost black colour. After two years in seawater, the filament lightened and lost its lustre. These observations have been made previously on basalt fibre composites aged in seawater and alkaline solutions (Wei et al., 2011; Wu et al., 2015).

The surfaces of the samples have also been analysed by SEM both in the initial state and after 7 months' immersion. Examples of these observations are presented on Figure 4. Figure 4 a shows the initial surface of the basalt fibres before ageing. The surface was smooth and clean with no defects. After 7 months at 15°C in seawater, the surface of the samples has changed and blisters have appeared. These were aligned in the fibre direction, and present on all fibres. Fibres immersed at 40°C in seawater during 7 months show holes, debonds, and crystals have formed on their surface as depicted in Figure 4 c. Different crystal patterns were observed. For fibres aged in 40°C deionized water, presented on Figure 4 d, the observations were the same as for the fibres immersed at the same temperature in seawater with crystals and debonds.

On Figure 4 c and d the shaded area represents one of the debonds observed during the analysis, it is then possible to see a degraded layer with a thickness of less than 1 micron. Several authors observed

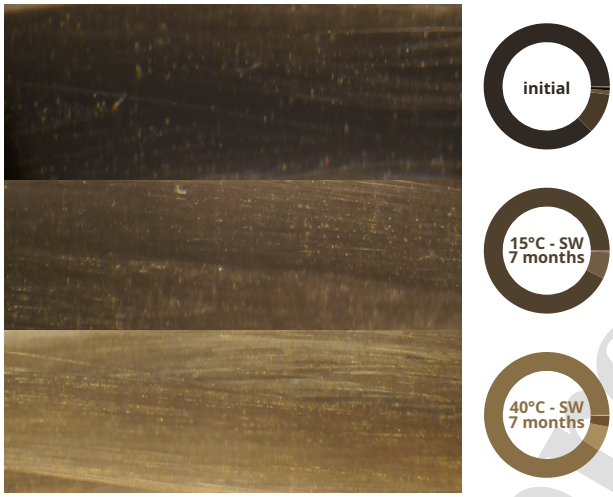

Figure 3: Change in colour observed for the basalt yarns after 7 months in seawater.

similar crystals formation and debonded layers on basalt fibres aged in alkaline solution (Scheffler et al., 2009; Rybin et al., 2016; Tang et al., 2018).

3.1.4. Composition analysis

EPMA has been used on 10 different fibres to characterize the composition of the fibre at the initial state. The initial composition obtained is summarized in Table 6 below.

	P_2O_5	Na_2O	MgO	SiO_2	Al_2O_3	K_2O	CaO	TiO_2	Fe_2O_3	Cr_2O_3	MnO	NiO
initial	0.3	2.0	3.9	54.3	17.4	1.7	8.2	1.1	9.8	0.005	0.2	0.002

Table 6: Initial composition of basalt fibre.

EDS has also been utilized in conjunction with SEM observations, in order to observe alterations in morphology. Figure 5 presents the results of two composition analyses conducted on fibres aged for 7 months at 40°C in seawater, with the initial composition included for comparison purposes. Crystals observed in Figure 4 (c) were analysed and labelled as "A", while a crystal-free surface was also analysed and marked as "B." In both areas, a significant decrease in SiO_2 content was observed, with less than 10% remaining on the surface lacking crystallization. Furthermore, an enrichment of Fe_2O_3, CaO, and TiO_2 was detected. The changes observed by EDS were more pronounced in the zone without crystalline structures. It is important to note that the analyses were performed on non-flat surfaces, which cannot therefore be used for quantitative comparisons. However, the observed magnitude of changes allows qualitative assessments to be made.

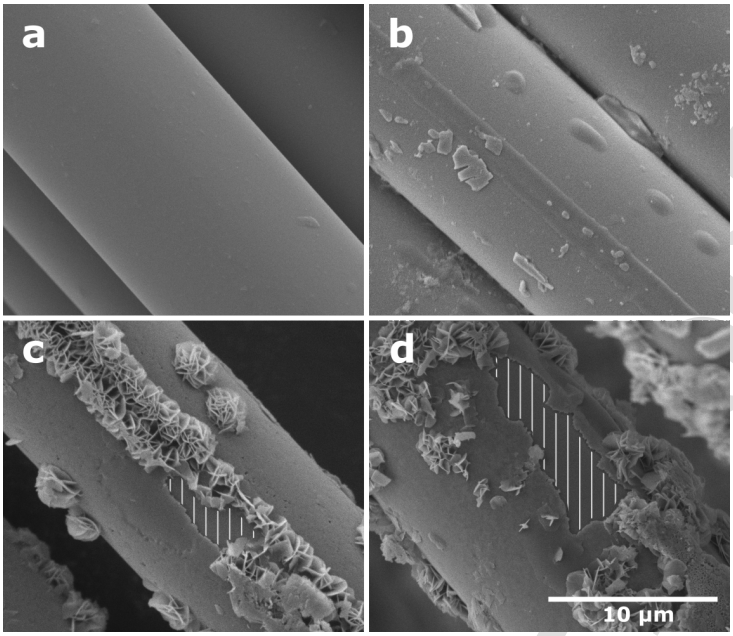

Figure 4: SEM observations of basalt fibres : a) at the initial state, b) after 7 months of immersion in a 15°C seawater, c) after 7 months of immersion in a 40°C seawater, d) after 7 months of immersion in a 40°C deionized water.

3.2. Composites

3.2.1. Water uptake

The laminates described in Table 3 were immersed in seawater at various temperatures: 4°C, 25°C, 40°C, and 60°C. The mass gain of three samples was regularly monitored for one year, and then observed occasionally over a longer period as the samples were immersed for 7.5 years.

Figure 6 shows the composite samples when they were removed from water after 7.5 years' immersion. There is a clear colour change, particularly marked at 60°C, for composites with both fibres. After 7.5 years in 40°C seawater, the basalt fibres appear to be lighter and orange at certain locations. After 7.5 years at 25°C, basalt fibres inside basalt/epoxy samples were looking slightly lighter. No change in the colour were observed for samples immersed at 4°C.

Figure 7 illustrates the different water absorption curves for each temperature. Table 7 presents the diffusion coefficients obtained by Davies and Verbouwe (2018) and updated mass at saturation. As the temperature rises, the diffusion coefficient shows an increase. At temperatures below 60°C, the mass at saturation ranges from 1.22% to 1.55% for both materials. However, at 60°C, saturation is not reached for either material, and the water content in the material increases rapidly.

One sample of basalt/epoxy composite aged at each temperature was then dried in an oven at 40°C. Figure 8 shows the desorption plots. The desorption rates are equivalent for both materials and across the different immersion temperatures. No loss of material was observed after 4 months of drying at 40°C.

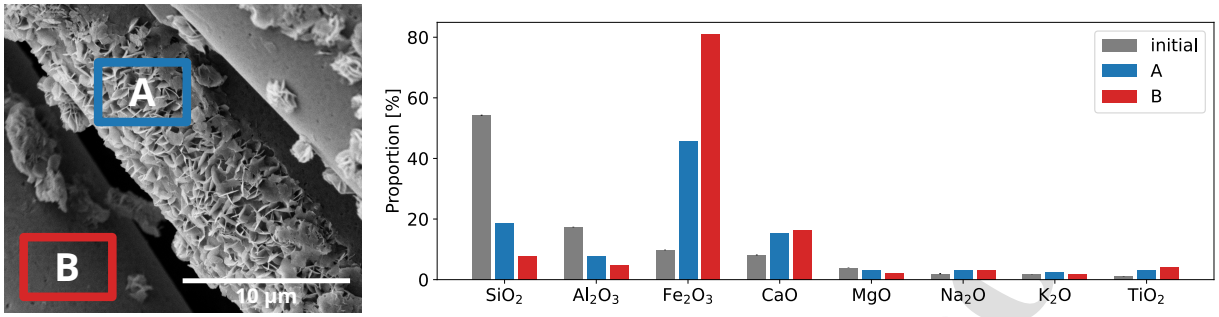

Figure 5: EDS analysis of basalt fibre surface after 7 months in seawater.

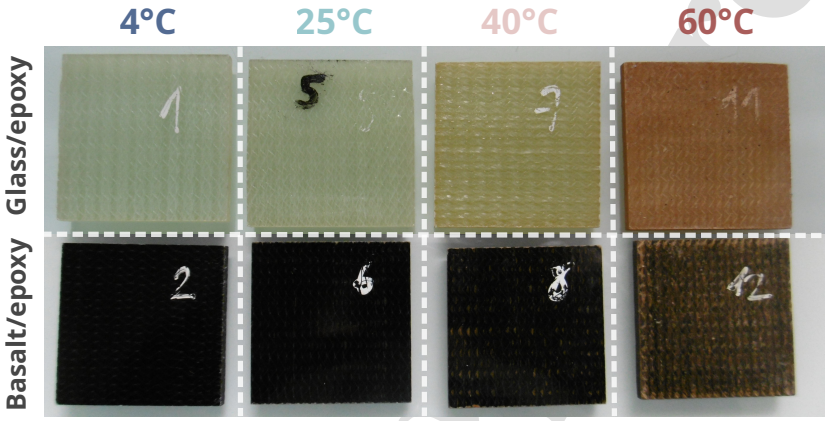

Figure 6: Weight gain samples after 7.5 years' immersion at 4 temperatures.

3.2.2. ILSS tests

The basalt/epoxy and glass/epoxy composites used for weight gain measurements were cut into interlaminar shear test specimens following the ASTM D2344 standard and tested to failure. The first tests were performed on samples in their initial state and then after saturation in seawater for 200 days at 40°C (Davies and Verbouwe, 2018). The results obtained for these two laminates are presented in Table 8.

In the initial state, the glass/epoxy composite exhibited higher interlaminar shear strength, with a failure stress of 48.0 MPa, while the basalt composite failed at 44.1 MPa. After saturation, both laminates experienced approximately a 20% reduction in strength.

3.2.3. Long term seawater ageing

Basalt/epoxy and E-glass/epoxy samples were retrieved after 7.5 years of ageing in seawater at various temperatures. To investigate the influence of ageing after saturation, these samples were subjected to the same testing method as the initial interlaminar shear strength (ILSS) tests. Figure 9 presents the results for the maximum τ_{13} obtained. The bars labelled as "initial" represent the ILSS values obtained in the saturated state after 200 days at 40°C.

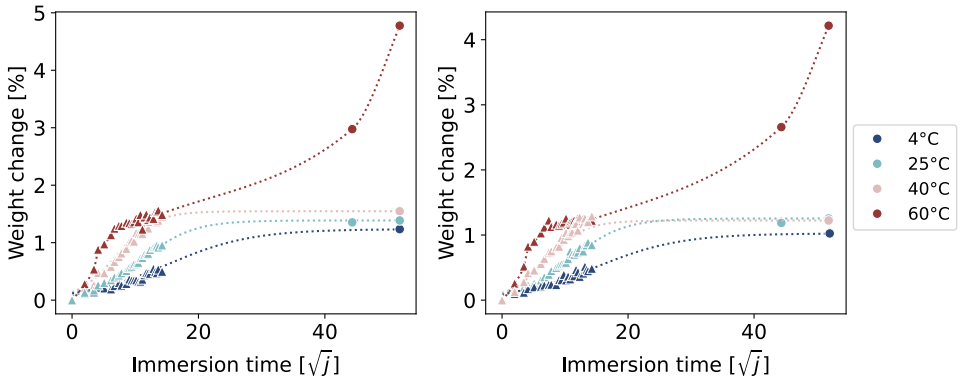

Figure 7: Weight change at different temperature for a) basalt/epoxy, and b) E-glass/epoxy. (▲): (Davies and Verbouwe, 2018), (●): present study

$m^2/s \times 10^{-12}$	4°C	25°C	40°C	60°C
Basalt/epoxy	2.4 (0.3)	7.0 (0.8)	19 (2)	79 (5)
	1.24%	1.39%	1.55%	4.78%
E-glass/epoxy	1.8 (0.8)	7.5 (0.7)	21 (1)	96 (8)
	1.24%	1.25%	1.22%	4.22%

Table 7: Weight change at different temperature for basalt/epoxy and E-glass/epoxy

At 4°C, the ILSS of the basalt/epoxy composite exhibited a -7% reduction, while the E-glass/epoxy composite showed no significant change in strength, experiencing a -2% loss. When immersed in seawater at 25°C, the ILSS of the basalt/epoxy composite decreased by -25%, whereas the E-glass/epoxy composite maintained its strength with a non-significant loss of -2%. As the temperature increased to 40°C, the reduction in ILSS became more pronounced. The basalt/epoxy composite experienced a -25% decrease, while the E-glass/epoxy composite also displayed a slight loss in strength, decreasing by -8%. At the highest temperature of 60°C, both composites demonstrated similar reductions in ILSS, with the basalt/epoxy composite showing a larger decrease of -39% compared to the -30% loss observed in the glass/epoxy composite.

3.2.4. SEM observations

Polished cross-sections of basalt/epoxy composite samples were prepared to examine potential morphological changes occurring due to prolonged contact between the fibre and seawater-saturated resin. Figure 10 displays the observations made for a sample aged for 7.5 years at 40°C, specifically focusing on the composite/seawater interface. The balanced nature of the composite allowed us to observe both normal and longitudinal sections.

A degradation gradient of the fibres is observable between the outer region of the composite in contact

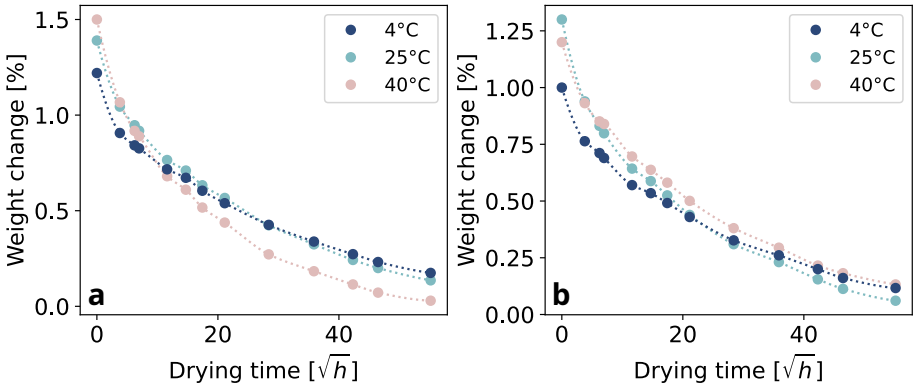

Figure 8: Water desorption after 7.5 years' immersion at 4 temperatures for a) basalt/epoxy, and b) E-glass/epoxy.

	τ_{13} [MPa]	τ_{13} saturated [MPa]	$\Delta\tau_{13}$
Basalt/epoxy	44.1 (1.7)	34.3 (0.7)	-22%
E-glass/epoxy	48.0 (1.6)	38.7 (0.7)	-19%

Table 8: τ_{13} for dry samples and samples saturated after 200 days at 40°C in renewed seawater according Davies and Verbouwe (2018).

with seawater and the inner region within the first 30 microns. This degradation gradient is more significant for the fibres exposed at a 90° angle, and degradation effects are visible up to 80 microns into the composite. At the lower left of Figure 10 (a), a crack between two degraded fibres can be observed. The altered fibres consist of two distinct parts: a heavily degraded outer layer and an apparently intact core. This surface degradation has been observed previously by several authors after immersion in an alkaline medium (Förster et al., 2014; Scheffler et al., 2009). At certain locations, the degraded layer appears to have been leached or washed away by seawater.

3.2.5. EPMA

EPMA analyses were conducted on the visible degradation features after 7.5 years of ageing in seawater at 40°C. Both the intact core of the fibre and the altered layer were examined to study the composition evolution with degradation and to compare the results with those obtained from individual fibres. Table 9 presents the compositions at the fibre core and in the outer degraded layer.

The analysis of the fibre core shows a composition similar to the initial composition. However, significant changes are observed for the altered layer. For instance, the silica content decreases to 1.50% of the altered composition, while the iron oxide content increases and represents almost 30% of the total composition. The titanium oxide content also enriches, increasing from 1.11% to 3.83%. Contrary to the EDS observations,

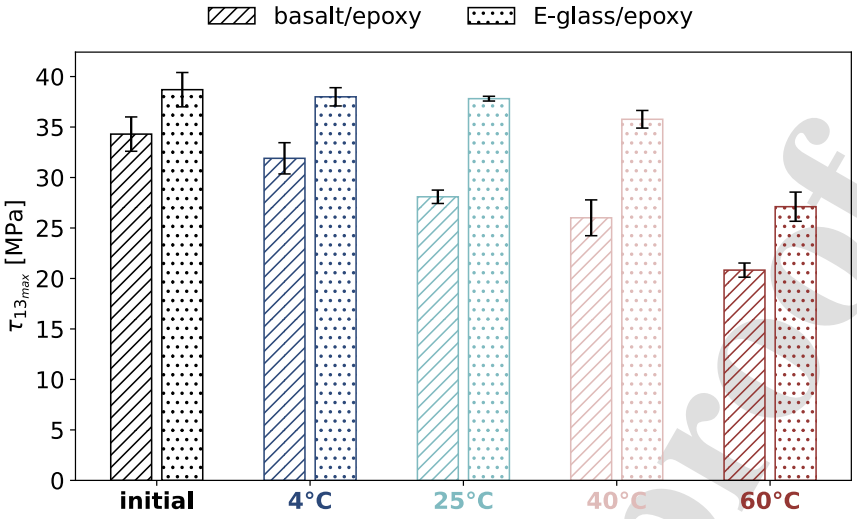

Figure 9: Mean residual τ_{13} after 7.5 year of ageing in renewed seawater at different temperatures.

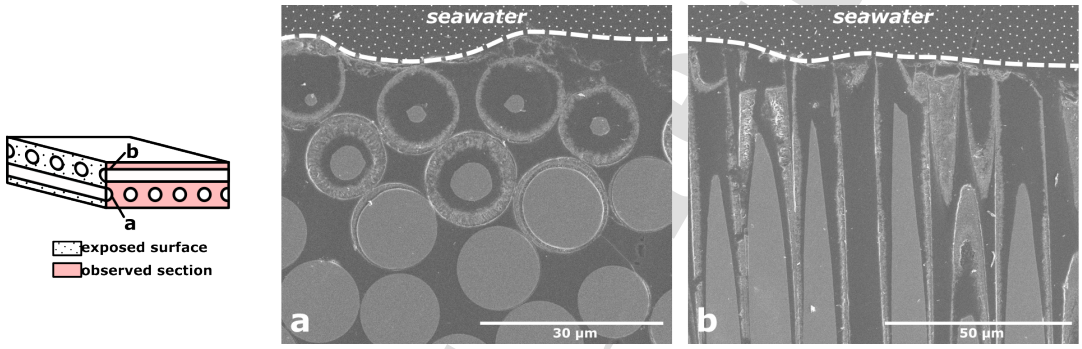

Figure 10: Cross (a) and longitudinal (b) sections of basalt fibres inside the epoxy matrix after 7.5 years of ageing in seawater at 40°C.

calcium oxide is no longer represented in the degraded part. Additionally, a substantial rise in magnesium oxide is observed, which was not evident in EDS results. Regarding silica, iron oxide, and titanium oxide, the EPMA findings align with the EDS results, providing consistent and complementary information.

4. Discussion

4.1. Fibre yarn degradation

Twenty samples of basalt fibres were tested to characterize the material in its initial state. The resulting strain-stress curves from these tests are shown in Figure 1, while the mechanical properties obtained for these basalt fibres are presented in Table 4. Values from the literature are provided in Table 10 below for comparison and discussion of the results.

	P_2O_5	Na_2O	MgO	SiO_2	Al_2O_3	K_2O	CaO	TiO_2	Fe_2O_3	Cr_2O_3	MnO	NiO
core	0.30	2.1	4.1	53.3	17.4	1.62	8.1	1.11	9.9	0.02	0.2	0
layer	0.37	0.13	21.7	1.50	11.6	0.02	0.48	3.83	28.7	0	0.06	0

Table 9: Fibre composition in the core and in the degraded outer layer after 7.5 years at 40°C [%].

The average Young's modulus obtained here, at 90 GPa, correlates well with values reported by various authors, which are also close to 90 GPa. However, for the properties at failure, the comparison with literature values is not as straightforward as for stiffness.

Tensile strength and elongation at break vary significantly among publications, with some authors reporting tensile strengths almost five times higher than others. This wide variation can be attributed to the difficulty in testing this fragile material, which is sensitive to defects and testing conditions. This could explain why the Young's moduli are similar, but the properties at failure differ.

Additionally, the strength of basalt fibres is influenced by their thermal history (Sabet, 2015), and thus, their manufacturing process plays a crucial role. Furthermore, the composition of basalt also affects its mechanical properties (Austin and Subramanian, 1979). Currently, there is no robust classification of basalt fibres similar to that used for glass fibres.

E [GPa]	$\epsilon_{failure}$ [%]	$\sigma_{failure}$ [MPa]	Reference
		1846	Sabet (2015)
76	2.56	992	Sim et al. (2005)
76	1.8 - 3.2	1400 - 2500	Fiore et al. (2011)
80 - 90		1350 - 4750	Chairman and Kumaresh Babu (2013)
		1371 - 1489	Militky and Kovacic (1996)
90	3.15	4800	Lopresto et al. (2011)
93 - 110	3.1 - 6.0	3000 - 4840	Militký et al. (2018)
57.3	3.93	2250	Lu et al. (2022)

Table 10: Mechanical properties of basalt fibres published in the literature.

Basalt fibres being sensitive to their surrounding environment, ageing tests were conducted in seawater at 15°C and 40°C, and in deionized water at 40°C. Figure 2 presents the change in tensile strength obtained over a 7-month monitoring period.

Basalt fibres experienced a significant drop in their strength within the first month of immersion in seawater. This sudden loss of properties was followed by a stabilization at a plateau, which is dependent on the temperature but not on the environment, as observed for the ageing at 40°C. Similar stabilization at a comparable level has been reported by Wu et al. (2015) for ageing in both saltwater and tap water.

Several authors suggested a passive degradation layer forms and acts as a protective barrier slowing down the degradation process of the fibres (Techer et al., 2001; Förster et al., 2014). This would explain the plateau in strength loss. Wei et al. (2011) attributed the degradation of basalt to the oxidation of iron present in the fibres by chloride complexes formed from Cl^- ions present in saltwater. However, in the present study, the plateau level is the same after ageing in natural seawater rich in ions and ageing in ultra-pure water where no ions are present. This suggests that the presence of Cl^- ions in the environment does not significantly impact the ageing rate nor the plateau reached. Therefore, the ageing of basalt fibres is governed by mechanisms other than the presence of chloride ions in the environment.

In addition to the loss of mechanical properties, changes in colour and a loss of lustre have been observed, as shown in Figure 3. To gain a better understanding of the surface mechanisms at play in the fibres, SEM analyses were conducted. The observations from these analyses after 7 months of immersion in the three environments are presented in Figure 4. After 7 months at 15°C, the observed surfaces displayed aligned bubbles or blistering, which can be considered as precursors of corrosion, potentially explaining the observed loss of properties at this temperature. After 7 months of immersion in both seawater and deionized water, the surface is altered, with the presence of debonds, holes, and crystal development. This kind of surface modification has been observed previously by several authors (Rybin et al., 2016; Scheffler et al., 2009; Tang et al., 2018; Wang et al., 2021a). The peeling of the corrosion layer does not seem to affect its protective role regarding the stability of the mechanical properties after 11 months of immersion at 40°C for both seawater and deionized water. Debonds are either negligible because they are very localised, or a new protective layer of oxidation forms very quickly following debonding. EDS analysis was used to investigate the degradation products present at the surface of the fibres. Both crystals and altered layers have been analysed, and the results are presented on Figure 5. The large proportion of iron oxides on the outside of the fibre could be linked to the oxidation of iron ions after glass network dissolution as observed by (Förster et al., 2014), but could also be explained by a migration of iron ions outside the glass network as described by Michelin et al. (2013). Similar iron oxide crystal patterns were observed by (Li et al., 2006). The corrosion shell was detected despite the absence of crystals on the surface, exhibiting an even higher iron content. This observation highlights the possibility that the layer could envelop the entire fibre, thereby confirming the hypothesis that a protective corrosion layer has indeed developed. But while this layer could protect the fibre from further degradation, it could also degrade the fibre-matrix interface when the fibre is used to reinforce a composite.

4.2. Basalt composite durability

Basalt/epoxy and glass/epoxy composites have been immersed in seawater for 7.5 years at different temperatures and weighed over time. The slopes of the weight gain curves on Figure 7 demonstrate that the saturation rate increases with the immersion temperature as expected and that the saturation plateau

remains nearly the same for each temperature below 60°C. At that temperature, a similar initial plateau is first observed, but followed by a continuous increase in water absorption. The glass transition temperature of the dry resin ranges between 75°C and 80°C (Davies and Verbouwe, 2018). Water saturation is known to decrease this temperature by approximately 20°C for epoxy resins due to plasticization (Le Guen-Geffroy et al., 2019). With an ageing temperature of 60°C, which is close to or above the glass transition temperature of the wet resin, prolonged immersion at this temperature could potentially result in chemical degradation of the matrix and yellowing, as evidenced in Figure 6 (Antoon and Koenig, 1981; Krauklis and Echtermeyer, 2018). The continuous water uptake by both composites regardless of the fibre could be explained by an increase in cracks and defects within the matrix, allowing water to penetrate more easily. This degradation led to an important loss of mechanical properties for both composites as seen on ILSS tests after 7.5 years of ageing at this temperature and makes it impossible to interpret the results regarding the degradation of the fibres themselves. The absence of matrix degradation at lower temperatures suggests that these conditions are more pertinent for assessing potential changes in the fibers or their interfaces. The discussion will therefore focus on the temperatures below 60°C. For these temperatures, the fact that the weight change plateaus are similar confirms the hypothesis that the mass at saturation can be described as independent of the immersion temperature, even at 4°C. Furthermore, the water absorption appears to be almost completely reversible for all temperatures, after 4 months of drying at 40°C, no loss of material is apparent. The observed color change in the samples at both 25°C and 40°C, initially attributed to the presence of iron oxides based on fibre results, appears to come from a very thin oxidized layer. This thin oxidized layer, while showing minimal impact on weight gain based on desorption curves, seems to affect the mechanical properties of the composites. After 7.5 years of immersion in natural seawater at 25°C and 40°C, the basalt/epoxy composites experienced respectively 18% and 25% reductions in their interlaminar shear strength. This decline indicates a loss in adhesion between the fibre and matrix at both temperatures, suggesting that the presence of the oxidized layer is responsible for degrading the fibre-matrix interface. This assumption is supported by the results obtained on the E-glass/epoxy composites where only a slight decrease of -8% was observed after 7.5 years at 40°C, which could be explained by the hydrolysis of the bond at the interface as observed by Devine et al. (2023). However, the decline in the mechanical properties observed on basalt/epoxy composites is small in comparison with the loss observed on the fibre alone, suggesting a protective role of the matrix as noted by other authors (Wu et al., 2015; Quagliarini et al., 2016; Lu et al., 2022). The matrix protective role has been investigated by SEM observations of the composite section that was in contact with seawater with results presented on Figure 10. Heavily degraded fibres were then observed at the seawater/composite interface, EPMA analysis revealed similar degradation products rich in iron oxides with almost no presence of silica, suggesting that the basalt alteration was similar in both experiments. Furthermore, the presence of a fibre degradation gradient indicates that the matrix has slowed down the diffusion of water within the composite, thus slowing down the degradation process observed on fibres in direct contact with seawater. However,

water diffusion seems to be faster in the degraded regions and in cracks, which leads to an acceleration of the degradation process as suggested by the degradation of the fibre near the crack seen on Figure 10 (a), and on the longitudinal degradation observed on all fibres on Figure 10 (b). Corrosion at the surface of the fibres not only reduces the fatigue life of basalt composites (Wang et al., 2019), but also accelerates degradation by allowing water to enter via the degraded layer or cracks. Corrosion on the surface of the fibres has a dual impact: it reduces the fatigue life of basalt composites, as discussed by Wang et al. (2019), and accelerates degradation by enabling water diffusion through deteriorated layers or cracks. These interlinked processes can combine, causing a quicker decline in mechanical properties under real-use conditions compared to samples aged without mechanical stress.

5. Conclusion

This paper describes a study on the long term behaviour of basalt fibres and their epoxy reinforced composites in natural seawater. The reinforcement alone was studied first and a fibre surface degradation mechanism was identified. This was shown to be accompanied by the development of iron oxide (Fe_20_3) degraded layer during seawater ageing and a significant loss in fibre tensile properties. The degradation in mechanical properties being significant even at low temperatures, it must be considered for applications where basalt fibres are used uncoated and immersed, such as rope for fishing gear.

However, this loss is not directly transferred to reinforced epoxy composites, for which the reduction in ILSS properties after 7.5 years in 40°C seawater is only around 20%. The polymer matrix provides long term protection to the fibres which show a long term stability in composite form. These findings illustrate the advantages gained by isolating the fibers from seawater using the matrix. However, they also highlight the necessity of examining degradation of basalt/epoxy composites under realistic operational conditions.

CRediT authorship contribution statement

Louis Le Gué: Conceptualization, data gathering and investigation, formal analysis, visualization, writing – original draft, writing - review and editing.

Peter Davies: Conceptualization, data gathering and investigation, formal analysis, writing – original draft, writing - review and editing.

Mael Arhant: Conceptualization, investigation, formal analysis, writing - review and editing.

Benoit Vincent: Conceptualization, investigation, writing - review and editing.

Wouter Verbouwe: Conceptualization, investigation, writing - review and editing.

Declaration of competing interest

The authors received materials from Basaltex, and Wouter Verbouwe is an employee of Basaltex. Nevertheless, these affiliations did not influence the design, interpretation, or reporting of the findings.

Acknowledgements

The authors would like to thank Nicolas Gayet for providing the SEM images and his expertise in the use of the scanning electron microscope, Jessica Langlade for performing EPMA analysis, and Mickael Rovere for his help with the preparation of polished cross-sections.

References

Antoon, M.K., Koenig, J.L., 1981. Irreversible effects of moisture on the epoxy matrix in glass-reinforced composites. Journal of Polymer Science: Polymer Physics Edition 19, 197–212. URL: https://onlinelibrary.wiley.com/doi/10.1002/pol.1981.180190202, doi:10.1002/pol.1981.180190202.

Austin, H.F., Subramanian, R.V., 1979. Method for forming basalt fibers with improved tensile strength. URL: https://patents.google.com/patent/US4149866/en.

Burkhard, D.J.M., Scherer, T., 2006. Surface oxidation of basalt glass/liquid. Journal of Non-Crystalline Solids 352, 241–247. URL: https://www.sciencedirect.com/science/article/pii/S0022309305008045, doi:10.1016/j.jnoncrysol.2005.11.029.

Chairman, C.A., Kumaresh Babu, S.P., 2013. Mechanical and abrasive wear behavior of glass and basalt fabric-reinforced epoxy composites. Journal of Applied Polymer Science 130, 120–130. URL: https://onlinelibrary.wiley.com/doi/abs/10.1002/app.39154, doi:10.1002/app.39154.

Chowdhury, I.R., Pemberton, R., Summerscales, J., 2022. Developments and Industrial Applications of Basalt Fibre Reinforced Composite Materials. Journal of Composites Science 6, 367. URL: https://www.mdpi.com/2504-477X/6/12/367, doi:10.3390/jcs6120367.

Davies, P., Verbouwe, W., 2018. Evaluation of Basalt Fibre Composites for Marine Applications. Applied Composite Materials 25, 299–308. URL: https://doi.org/10.1007/s10443-017-9619-3, doi:10.1007/s10443-017-9619-3.

Devine, M., Bajpai, A., Obande, W., Ó Brádaigh, C.M., Ray, D., 2023. Seawater ageing of thermoplastic acrylic hybrid matrix composites for marine applications. Composites Part B: Engineering 263, 110879. URL: https://linkinghub.elsevier.com/retrieve/pii/S1359836823003827, doi:10.1016/j.compositesb.2023.110879.

Fiore, V., Di Bella, G., Valenza, A., 2011. Glass–basalt/epoxy hybrid composites for marine applications. Materials & Design 32, 2091–2099. URL: https://www.sciencedirect.com/science/article/pii/S0261306910006692, doi:10.1016/j.matdes.2010.11.043.

Fiore, V., Scalici, T., Di Bella, G., Valenza, A., 2015. A review on basalt fibre and its composites. Composites Part B: Engineering 74, 74–94. URL: https://linkinghub.elsevier.com/retrieve/pii/S1359836815000062, doi:10.1016/j.compositesb.2014.12.034.

Förster, T., Scheffler, C., Mäder, E., Heinrich, G., Jesson, D.A., Watts, J.F., 2014. Dissolution behaviour of model basalt fibres studied by surface analysis methods. Applied Surface Science 322, 78–84. URL: https://www.sciencedirect.com/science/article/pii/S0169433214022971, doi:10.1016/j.apsusc.2014.10.058.

Jiang, T., Wang, Y., Shi, S., Yuan, N., Wu, X., Shi, D., Sun, K., Zhao, Y., Li, W., Yu, J., 2022. Study on compressive strength of lightweight concrete filled with cement-reinforced epoxy Macrospheres and basalt fibers. Structures 44, 1347–1355. URL: https://linkinghub.elsevier.com/retrieve/pii/S2352012422007093, doi:10.1016/j.istruc.2022.08.056.

Krauklis, A., Echtermeyer, A., 2018. Mechanism of Yellowing: Carbonyl Formation during Hygrothermal Aging in a Common Amine Epoxy. Polymers 10, 1017. URL: http://www.mdpi.com/2073-4360/10/9/1017, doi:10.3390/polym10091017.

Le Guen-Geffroy, A., Le Gac, P.Y., Habert, B., Davies, P., 2019. Physical ageing of epoxy in a wet environment: Coupling between plasticization and physical ageing. Polymer Degradation and Stability 168, 108947. URL: https://linkinghub.elsevier.com/retrieve/pii/S0141391019302678, doi:10.1016/j.polymdegradstab.2019.108947.

Li, F.b., Chen, J.j., Liu, C.s., Dong, J., Liu, T.x., 2006. Effect of iron oxides and carboxylic acids on photochemical degradation of bisphenol A. Biology and Fertility of Soils 42, 409–417. URL: https://doi.org/10.1007/s00374-006-0084-7, doi:10.1007/s00374-006-0084-7.

Lopresto, V., Leone, C., De Iorio, I., 2011. Mechanical characterisation of basalt fibre reinforced plastic. Composites Part B: Engineering 42, 717–723. URL: https://www.sciencedirect.com/science/article/pii/S1359836811000588, doi:10.1016/j.compositesb.2011.01.030.

Lu, C., Ni, M., Chu, T., He, L., 2020. Comparative Investigation on Tensile Performance of FRP Bars after Exposure to Water, Seawater, and Alkaline Solutions. Journal of Materials in Civil Engineering 32, 04020170. URL: https://ascelibrary.org/doi/10.1061/%28ASCE%29MT.1943-5533.0003243, doi:10.1061/(ASCE)MT.1943-5533.0003243.

Lu, Z., Jiang, M., Pan, Y., Xian, G., Yang, M., 2022. Durability of basalt fibers, glass fibers, and their reinforced polymer composites in artificial seawater. Polymer Composites 43, 1961–1973. URL: https://4spepublications.onlinelibrary.wiley.com/doi/10.1002/pc.26511, doi:10.1002/pc.26511.

Michelin, A., Burger, E., Rebiscoul, D., Neff, D., Bruguier, F., Drouet, E., Dillmann, P., Gin, S., 2013. Silicate Glass Alteration Enhanced by Iron: Origin and Long-Term Implications. Environmental Science & Technology 47, 750–756. URL: https://pubs.acs.org/doi/10.1021/es304057y, doi:10.1021/es304057y.

Militky, J., Kovacic, V., 1996. Ultimate Mechanical Properties of Basalt Filaments. Textile Research Journal 66, 225–229. URL: http://journals.sagepub.com/doi/10.1177/004051759606600407, doi:10.1177/004051759606600407.

Militky, J., Kovacic, V., Rubnerova, J., 2002. Influence of thermal treatment on tensile failure of basalt fibers. Engineering Fracture Mechanics 69, 1025–1033. URL: https://www.sciencedirect.com/science/article/pii/S0013794401001199, doi:10.1016/S0013-7944(01)00119-9.

Militký, J., Mishra, R., Jamshaid, H., 2018. Basalt fibers, in: Handbook of Properties of Textile and Technical Fibres. Elsevier, pp. 805–840. URL: https://linkinghub.elsevier.com/retrieve/pii/B9780081012727000201, doi:10.1016/B978-0-08-101272-7.00020-1.

Millero, F.J., Feistel, R., Wright, D.G., McDougall, T.J., 2008. The composition of Standard Seawater and the definition of the Reference-Composition Salinity Scale. Deep Sea Research Part I: Oceanographic Research Papers 55, 50–72. URL: https://www.sciencedirect.com/science/article/pii/S0967063707002282, doi:10.1016/j.dsr.2007.10.001.

Quagliarini, E., Monni, F., Bondioli, F., Lenci, S., 2016. Basalt fiber ropes and rods: Durability tests for their use in building engineering. Journal of Building Engineering 5, 142–150. URL: https://linkinghub.elsevier.com/retrieve/pii/S2352710215300553, doi:10.1016/j.jobe.2015.12.003.

Rybin, V.A., Utkin, A.V., Baklanova, N.I., 2016. Corrosion of uncoated and oxide-coated basalt fibre in different alkaline media. Corrosion Science 102, 503–509. URL: https://www.sciencedirect.com/science/article/pii/S0010938X15301451, doi:10.1016/j.corsci.2015.11.004.

Sabet, S., 2015. The Effect of Thermal Treatment on Tensile Properties of Basalt Fibers. Journal of Ceramic Science and Technology 6, 245–248. URL: https://doi.org/10.4416/JCST2014-00053, doi:10.4416/JCST2014-00053.

Scheffler, C., Förster, T., Mäder, E., Heinrich, G., Hempel, S., Mechtcherine, V., 2009. Aging of alkali-resistant glass and basalt

fibers in alkaline solutions: Evaluation of the failure stress by Weibull distribution function. Journal of Non-Crystalline Solids 355, 2588–2595. URL: https://linkinghub.elsevier.com/retrieve/pii/S0022309309006322, doi:10.1016/j.jnoncrysol.2009.09.018.

Sim, J., Park, C., Moon, D.Y., 2005. Characteristics of basalt fiber as a strengthening material for concrete structures. Composites Part B: Engineering 36, 504–512. URL: https://www.sciencedirect.com/science/article/pii/S1359836805000454, doi:10.1016/j.compositesb.2005.02.002.

Tang, C., Jiang, H., Zhang, X., Li, G., Cui, J., 2018. Corrosion Behavior and Mechanism of Basalt Fibers in Sodium Hydroxide Solution. Materials 11, 1381. URL: http://www.mdpi.com/1996-1944/11/8/1381, doi:10.3390/ma11081381.

Techer, I., Advocat, T., Lancelot, J., Liotard, J.M., 2001. Dissolution kinetics of basaltic glasses: control by solution chemistry and protective effect of the alteration film. Chemical Geology 176, 235–263. URL: https://www.sciencedirect.com/science/article/pii/S0009254100004009, doi:10.1016/S0009-2541(00)00400-9.

Wang, Q., Yan, T., Ding, L., 2021a. Effect of Seawater Environment on the Structure and Performance of Basalt Continuous Fiber. Materials 14, 1862. URL: https://www.mdpi.com/1996-1944/14/8/1862, doi:10.3390/ma14081862. number: 8 Publisher: Multidisciplinary Digital Publishing Institute.

Wang, S., Wang, S., Li, G., Cui, J., 2021b. Dynamic response and fracture analysis of basalt fiber reinforced plastics and aluminum alloys adhesive joints. Composite Structures 268, 114013. URL: https://linkinghub.elsevier.com/retrieve/pii/S0263822321004736, doi:10.1016/j.compstruct.2021.114013.

Wang, X., Zhao, X., Wu, Z., 2019. Fatigue degradation and life prediction of basalt fiber-reinforced polymer composites after saltwater corrosion. Materials & Design 163, 107529. URL: https://www.sciencedirect.com/science/article/pii/S0264127518308724, doi:10.1016/j.matdes.2018.12.001.

Wei, B., Cao, H., Song, S., 2011. Degradation of basalt fibre and glass fibre/epoxy resin composites in seawater. Corrosion Science 53, 426–431. URL: https://www.sciencedirect.com/science/article/pii/S0010938X10004841, doi:10.1016/j.corsci.2010.09.053.

Wu, G., Wang, X., Wu, Z., Dong, Z., Zhang, G., 2015. Durability of basalt fibers and composites in corrosive environments. Journal of Composite Materials 49, 873–887. URL: https://doi.org/10.1177/0021998314526628, doi:10.1177/0021998314526628.

Xing, D., Xi, X.Y., Ma, P.C., 2019. Factors governing the tensile strength of basalt fibre. Composites Part A: Applied Science and Manufacturing 119, 127–133. URL: https://www.sciencedirect.com/science/article/pii/S1359835X19300375, doi:10.1016/j.compositesa.2019.01.027.

Declaration of interests

☐The authors declare that they have no known competing financial interests or personal relationships that could have appeared to influence the work reported in this paper.

☒The authors declare the following financial interests/personal relationships which may be considered as potential competing interests:

Louis LE GUE reports equipment, drugs, or supplies was provided by Basaltex. Wouter Verbouwe reports a relationship with Basaltex that includes: employment.